

Noncontact temperature measurement. I. Interpolation based techniques

Mansoor A. Khan,^{a1} Charly Allemand, and Thomas W. Eagar
Massachusetts Institute of Technology, Cambridge, Massachusetts 02139

(Received 17 May 1990; accepted for publication 29 October 1990)

Various ratio pyrometry techniques (two, three, and four color) are analyzed and shown to possess hitherto unknown sources of error under certain conditions. These conditions are shown to arise quite frequently. The ratio method is shown to be better suited to the shorter wavelengths. It has been shown, for various emissivities, that the predicted temperature has an asymptote at some wavelength. Ratio pyrometry methods are shown to be very sensitive to measurement noise and this sensitivity grows quickly with the number of terms in the ratio. The effect of a reference temperature in the system is examined and it is shown that under certain conditions this reference temperature can be used to make accurate predictions regarding the temperature elsewhere in the system even if the emissivity changes.

I. INTRODUCTION

The accurate measurement and control of temperature can be of great importance in most materials manufacturing and processing applications. With present-day technology such measurement almost always requires either physical contact with the subject or an extensive calibration procedure. In many cases contact is either not desirable, because it may significantly alter the temperature or other characteristics of the subject, or is not possible, because the subject is moving, is too far away, is too hot or is in an otherwise hostile environment. Similarly calibration may not be possible if the characteristics change too much.

A prime example of a process in which physical contact is not desirable is the growth of silicon single crystals. The quality of the final crystal is very strongly dependent on both the purity of the metal and the convection velocity fields in the melt. These velocity fields in turn are a strong function of the temperature distribution within the melt. Here, it is undesirable to place a probe in contact with the melt because (a) it might affect the temperature and velocity fields, and (b) molten silicon is an excellent solvent of most materials and is therefore easily contaminated. Accurate temperature measurement is also important for many of the stages in the processing of both silicon and gallium-arsenide semiconductor devices, an example of this would be fast thermal processing. Additionally, the ever increasing demand for faster and smaller devices increases the importance of temperature control during processing.

In the steel industry continuous casting is an increasingly important process for the manufacture of steel plate and sheet. This is another process in which it is not possible to make effective contact with the plate, in this case because the plate is constantly moving. The American Iron and Steel Institute (AISI) estimated in 1982 that an accurate non-contact temperature sensor would save the industry about \$275 million per year.

Another example of an area requiring accurate temperature sensing is the jet engine industry. Aircraft engine manufacturers are increasingly concerned with very accurate temperature measurement and control in the engine. It has been estimated that a 5° rise in the temperature of certain critical components can lead to a 10% decline in engine life.

Similarly there are many applications in research and development where very accurate noncontact temperature measurement is required. One example is in welding research. The velocity fields within the molten puddle of metal underneath the arc are a strong function of the temperature distribution within the puddle. The final shape and integrity of the weld depend upon these velocity fields. It is therefore desirable to know the temperature distribution within the puddle. The physical size of the puddle and the large temperature gradients within it (1000 K/cm) make it impossible to use a contact method such as a thermocouple without affecting the temperature and velocity profiles within the puddle. Applications also exist in other research areas such as high temperature mechanical testing and high-temperature metallurgy.

All of these and many other processes would benefit from a noninvasive method of temperature measurement. Multiwavelength pyrometry may be the solution to this problem.

A. Basic theory

All bodies above absolute zero radiate thermal energy. The most efficient thermal radiator is a black body, which is defined as an object that will absorb all incident radiation. The Stefan-Boltzmann law describes the radiant emittance (W') of a black body in units of power per unit area of the source:

$$W' = \sigma T^4, \quad (1)$$

where T is the absolute temperature and σ is the Stefan-Boltzmann constant. A real body, however, emits only a fraction of what a black body emits at any given temperature. The total hemispherical emissivity is thus defined as

$$\epsilon = W/W', \quad (2)$$

where W is the radiant emittance of a real body. The radi-

^{a1} Present address: Wyman Gordon Co., 244 Worcester St., N. Grafton, MA 01536.

ance (N) of a source is defined as (the radiant emittance per solid angle)

$$N = W/\pi. \quad (3)$$

The radiance per unit wavelength, or spectral radiance for a black body is given by the Planck radiation law.

For a real body, Planck's equation must be modified by the inclusion of an emissivity term (ϵ_λ) to give Eq. (4) below

$$N_\lambda = \frac{\epsilon_\lambda C_1}{\lambda^5 [\exp(C_2/\lambda T) - 1]}, \quad (4)$$

where λ is the wavelength, T is the absolute temperature, and C_1 and C_2 are the Planck constants.

The emissivities of real bodies are functions of wavelength, temperature, and surface condition. For the purpose of this discussion the most important of these factors is wavelength. The emissivity can easily vary by 10% over fairly small wavelength ranges. Therefore any pyrometer that does not account for emissivity can produce significant errors. Because emissivity is rarely known for a given set of circumstances, it must be either measured or calculated separately if an accurate temperature determination is to be made.

Brightness pyrometers, which allow the operator to match the appearance of a heated, calibrated standard to the appearance of the object, attempt to solve the emissivity problem by making the standard of the same material as the object, but this tactic severely restricts the use of the device because it may not be possible to get a standard of the same material and surface condition. Furthermore the emissivity of the object can change quite rapidly as the environment and surface conditions change.

An improvement over the brightness pyrometer is the total radiation pyrometer. This instrument uses the Stefan-Boltzmann relation and measures the radiance electronically using a photodetector, but it still suffers from the inaccuracies caused by uncertainties in the emissivity determination. This device has the advantage of speed and compactness over the brightness pyrometer and is capable of measuring relative temperatures quite accurately.

Ratio or two-color pyrometers, on the other hand, can circumvent the emissivity measurement issue in certain specific cases. The two-color method uses an approximation of the Planck relation called the Wien radiation relation:

$$N_\lambda = \frac{\epsilon_\lambda C_1}{\lambda^5 \exp(C_2/\lambda T)}. \quad (5)$$

This approximation gives a deviation of less than 1% from the Planck law if

$$\lambda T < 3125 \mu\text{m K}.$$

The Wien relation can be solved for temperature at two different wavelengths to give:

$$T = \frac{C_2(\lambda_2 - \lambda_1)}{\{\lambda_1 \lambda_2 [5 \ln(\lambda_2/\lambda_1) - \ln(N_1/N_2) + \ln(\epsilon_1/\epsilon_2)]\}}. \quad (6)$$

If the wavelengths λ_1 and λ_2 are chosen such that gray body behavior can be assumed (i.e., $\epsilon_1 = \epsilon_2$), then the emissivity term drops out and the temperature calculation is

straight forward. The assumption of gray body behavior becomes more valid as $\Delta\lambda = (\lambda_1 - \lambda_2) \rightarrow 0$ but as $\Delta\lambda \rightarrow 0$ any errors in the radiance measurements become more significant. Increasing the separation of the wavelengths reduces the effects of radiance measurement errors but the gray body assumption becomes less valid.

To increase the accuracy of the device farther, the emissivity must be modeled better. This can be achieved by measuring the spectral radiance at a larger (> 2) number of wavelengths. The class of techniques called multiwavelength pyrometry is based upon such multiple radiance measurements. These techniques model the emissivity as a smooth function of wavelength having a number of undetermined parameters. Equation (4), using the emissivity model, is then curve fit to the experimental data to determine the values of the unknown parameters in the emissivity function and the temperature.

This document describes the results of a comprehensive study of the sources of error and the limitations of the ratio technique.

II. RATIO PYROMETRY

All multiwavelength pyrometry techniques work on the same principle: modeling the emitted radiance of a real body at a given temperature as the product of an emissivity and the theoretical radiant output of a black body as predicted by the Planck radiation law. Beyond that, these techniques can be divided into two general classes. Those in the first class, which we have chosen to call "interpolation based techniques" and which are being discussed here, make radiance measurements at $n + 1$ different wavelengths and model the emissivity as consisting of n undetermined parameters. The $n + 1$ equations thus generated are then used to calculate the temperature, either by eliminating the emissivity parameters or by calculating both the emissivity and the temperature. The second class of techniques, which we will refer to as "least-squares-based techniques," are only different from the previous class in that the radiance measurements are made at m wavelengths such that $m \gg n$ and the redundancy in the data is used to smooth out the effects of noise in the data. The least-squares technique will be discussed in greater detail in part II.

For now we shall concentrate on the interpolation based techniques. These can be further separated into two distinct approaches; those that use the data to eliminate the emissivity from the formulation and calculate only the temperature (referred to as ratio pyrometry); and those that explicitly calculate both the temperature and the n emissivity parameters by generating an $n + 1$ order interpolating polynomial.

The latter of these two approaches was first suggested by Svet.¹⁻³ The theoretical errors associated with this technique have been extensively analyzed by Coates⁴ and shown to be quite unacceptable for $n > 3$. Ratio pyrometry, on the other hand, has been around much longer. The theory and history of two, three, and four color ratio pyrometry has been given by Reynolds.⁵ We shall in this article attempt to investigate certain characteristics of Ratio Pyrometry, which to our knowledge have not been considered before.

A. Theory

The theory of ratio pyrometry is relatively simple in that it consists of building ratios to eliminate the emissivity when certain assumptions hold true.

1. Two color

The energy flux N_λ emitted by a real body in the wavelength range λ to $\lambda + d\lambda$ is given by Planck's law as

$$N_\lambda d\lambda = \frac{\epsilon_\lambda C_1 d\lambda}{\lambda^5 [\exp(C_2/\lambda T) - 1]} \\ = \epsilon_\lambda f(\lambda) d\lambda.$$

For a one color pyrometer the error in temperature as a function of the error in the radiance measurement and the emissivity estimate can be estimated from the differential form of this equation. This equation as derived by Hunter⁶ (among others) is listed below. Defining

$$A = C_2/\lambda T, \quad B = Ae^A/(e^A - 1),$$

$$\frac{dN_\lambda}{N_\lambda} = \frac{d\epsilon_\lambda}{\epsilon_\lambda} + \frac{BdT}{T},$$

the quantity B for our temperature (around 1800 K) and wavelength range (0.7–1.0 μm) is of the order of 10. This implies that a 10% error in radiance measurement or a 10% error in the emissivity estimate will cause at most a 1% error in the temperature estimate.

If we now take the ratio of the emitted energy fluxes centered on λ_1 and λ_2

$$R_{12} = \frac{N_1 d\lambda_1}{N_2 d\lambda_2} = \frac{\epsilon_1 f(\lambda_1) d\lambda_1}{\epsilon_2 f(\lambda_2) d\lambda_2}.$$

With equal bandwidths and with Wien's approximation, this results in

$$T = \frac{C_2 [(1/\lambda_2) - (1/\lambda_1)]}{\ln R_{12} - 5 \ln(\lambda_2/\lambda_1) - \ln(\epsilon_1/\epsilon_2)}.$$

The assumption of two color pyrometry is that $\epsilon_1 = \epsilon_2$, and so the apparent temperature (T_a) measured by the pyrometer is

$$T_a = \frac{C_2 [(1/\lambda_2) - (1/\lambda_1)]}{\ln R_{12} - 5 \ln(\lambda_2/\lambda_1)}.$$

The error of a two color pyrometer as given by Reynolds⁵ is

$$\frac{1}{T} - \frac{1}{T_a} = \frac{\lambda_1 \lambda_2}{C_2 (\lambda_2 - \lambda_1)} \ln\left(\frac{\epsilon_1}{\epsilon_2}\right). \quad (7)$$

From (7) we get

$$T_a = \frac{TC_2(\lambda_1 - \lambda_2)}{C_2(\lambda_1 - \lambda_2) + T\lambda_1\lambda_2 \ln(\epsilon_1/\epsilon_2)}.$$

If we now let $\lambda_1 = \lambda$, $\lambda_2 = \lambda + \Delta\lambda$, $\epsilon_1 = \epsilon$, and $\epsilon_2 = \epsilon + \Delta\epsilon$, then

$$T_a = \frac{TC_2\Delta\lambda}{C_2 - T\lambda(\lambda + \Delta\lambda) [\ln \epsilon - \ln(\epsilon + \Delta\epsilon)]}.$$

For a specific target temperature T

$$T_a = f(\lambda, \Delta\lambda, \epsilon, \Delta\epsilon),$$

$$dT_a = \frac{\partial T_a}{\partial \lambda} d\lambda + \frac{\partial T_a}{\partial \Delta\lambda} d\Delta\lambda + \frac{\partial T_a}{\partial \epsilon} d\epsilon + \frac{\partial T_a}{\partial \Delta\epsilon} d\Delta\epsilon. \quad (8)$$

Later on we shall see that the apparent temperature, as predicted by a two-color pyrometer tends to an asymptote under certain circumstances. This behavior can have two possible causes, i.e., the failure of the Wien approximation or the misbehavior of the terms in Eq. (8). At the wavelengths and temperatures in question ($< 1.1 \mu\text{m}$ and $< 2500 \text{ K}$) the Wien approximation is very good and does not cause any problems. The asymptotic behavior must therefore be caused by one or more of the terms in Eq. (8).

Assuming that the uncertainty at both the wavelengths (λ_1 and λ_2) is the same, we can show that

$$d\Delta\lambda \leq 2d\lambda, \quad d\Delta\epsilon \leq 2d\epsilon,$$

and if $(\Delta\epsilon/\Delta\lambda) = K$ then we have (for small enough $\Delta\lambda$ or if ϵ is linear in λ)

$$dT_a \leq \left(\frac{\partial T_a}{\partial \lambda} + 2 \frac{\partial T_a}{\partial \Delta\lambda} + K \frac{\partial T_a}{\partial \epsilon} + 2K \frac{\partial T_a}{\partial \Delta\epsilon} \right) d\lambda, \quad (9)$$

where K is generally less than 1.

2. Three color

Three-color pyrometry is also based on an algorithm similar to two-color pyrometry. Here we form two ratios, R_{12} and R_{32} , and after taking logarithms we get

$$\ln(R_{12}R_{32}) = \ln\left(\frac{\epsilon_1\epsilon_3}{\epsilon_2^2}\right) + 5 \ln\left(\frac{\lambda_2^2}{\lambda_1\lambda_3}\right) \\ + \frac{C_2}{T} \left[\left(\frac{\lambda_1 - \lambda_2}{\lambda_1\lambda_2}\right) - \left(\frac{\lambda_2 - \lambda_3}{\lambda_2\lambda_3}\right) \right] \\ + \ln\left(\frac{d\lambda_1 d\lambda_2}{d\lambda_2^2}\right).$$

If $d\lambda_1 = d\lambda_2 = d\lambda_3$, then

$$T = A/B,$$

where

$$A = C_2 \left[\left(\frac{\lambda_1 - \lambda_2}{\lambda_1\lambda_2}\right) - \left(\frac{\lambda_2 - \lambda_3}{\lambda_2\lambda_3}\right) \right], \\ B = \ln\left(\frac{R_{12}}{R_{23}}\right) - \ln\left(\frac{\epsilon_3}{\epsilon_2^2}\right) - 5 \ln\left(\frac{\lambda_2^2}{\lambda_1\lambda_3}\right).$$

Three-color pyrometry makes the assumption that

$$\epsilon_1\epsilon_3 = \epsilon_2^2,$$

and the temperature error in this case is given by

$$\frac{1}{T} - \frac{1}{T_a} = \frac{\lambda_1\lambda_2\lambda_3}{(\lambda_2 - \lambda_1)(\lambda_3 - \lambda_1)(\lambda_3 - \lambda_2)} \\ \times \left[\lambda_1 \ln\left(\frac{\epsilon_2}{\epsilon_3}\right) + \lambda_2 \ln\left(\frac{\epsilon_3}{\epsilon_1}\right) + \lambda_3 \ln\left(\frac{\epsilon_1}{\epsilon_2}\right) \right].$$

3. Four color

Similarly for four colors we make three ratios R_{12} , R_{23} , and R_{34}

$$\frac{R_{12}R_{34}}{R_{23}} = \frac{\epsilon_1 \epsilon_3^2}{\epsilon_2^2 \epsilon_4} \left(\frac{\lambda_2^2 \lambda_4}{\lambda_1 \lambda_3^2} \right)^5 \times \exp \left\{ \frac{C_2}{T} \left[\left(\frac{\lambda_1 - \lambda_2}{\lambda_1 \lambda_2} \right) + \left(\frac{\lambda_3 - \lambda_4}{\lambda_3 \lambda_4} \right) - \left(\frac{\lambda_2 - \lambda_3}{\lambda_2 \lambda_3} \right) \right] \right\},$$

which reduces to

$$T = A/B, \\ A = C_2 \left[\left(\frac{\lambda_1 - \lambda_2}{\lambda_1 \lambda_2} \right) + \left(\frac{\lambda_3 - \lambda_4}{\lambda_3 \lambda_4} \right) - \left(\frac{\lambda_2 - \lambda_3}{\lambda_2 \lambda_3} \right) \right], \\ B = \ln \left(\frac{R_{12}R_{34}}{R_{23}} \right) - \ln \left(\frac{\epsilon_1 \epsilon_3^2}{\epsilon_2^2 \epsilon_4} \right) - 5 \ln \left(\frac{\lambda_2^2 \lambda_4}{\lambda_1 \lambda_3^2} \right).$$

Four-color pyrometry gives the correct temperature if $\epsilon_1 \epsilon_3^2 = \epsilon_2^2 \epsilon_4$. The error for four color pyrometry is given by

$$\frac{1}{T} - \frac{1}{T_a} = \frac{\ln(\epsilon_1 \epsilon_3^2 / \epsilon_2^2 \epsilon_4)}{C_2 [(2/\lambda_2) - (1/\lambda_1) - (2/\lambda_3) + (1/\lambda_4)]}.$$

If we approximate

$$\epsilon_2 \sim \epsilon_3 - \Delta\epsilon, \quad \epsilon_4 \sim \epsilon_3 + \Delta\epsilon, \\ \frac{\epsilon_3 \epsilon_3}{\epsilon_2 \epsilon_4} = \frac{\epsilon_3^2}{\epsilon_3^2 - \Delta\epsilon^2} = \frac{1}{1 - \left(\frac{\Delta\epsilon}{\epsilon_3} \right)^2}, \quad \frac{\epsilon_3^2}{\epsilon_2 \epsilon_4} = 1$$

if $(\Delta\epsilon/\epsilon_3)^2 \ll 1$. Similarly with $\lambda_2 = \lambda_3 - \Delta\lambda$, and $\lambda_4 = \lambda_3 + \Delta\lambda$,

$$\frac{1}{\lambda_2} - \frac{1}{\lambda_3} + \frac{1}{\lambda_4} - \frac{1}{\lambda_3} \\ = \frac{1}{\lambda_3 - \Delta\lambda} - \frac{1}{\lambda_3} + \frac{1}{\lambda_3 + \Delta\lambda} - \frac{1}{\lambda_3} \\ = \frac{\lambda_3 - \lambda_3 + \Delta\lambda + \lambda_3 - \lambda_3 - \Delta\lambda}{\lambda_3(\lambda_3^2 - \Delta\lambda^2)} = 0.$$

So for four colors

$$\frac{1}{T} - \frac{1}{T_a} \cong \frac{\ln(\epsilon_1/\epsilon_2)}{C_2 [(1/\lambda_2) - (1/\lambda_1)]},$$

which is the same as the error for a two-color pyrometer as given by Eq. (7).

B. Measurement noise

If one were to assume that the effect of measurement noise in the radiance is an uncertainty in the associated emissivity, then Coates⁴ has shown that the error in the predicted temperature is given by

$$\frac{\Delta T_i}{T^2} = \frac{(1/C_2) (\prod_{j=1}^{n+1} \lambda_j) (\Delta\epsilon_i/\epsilon_i)}{\prod_{j=1, j \neq i}^{n+1} (\lambda_j - \lambda_i)}, \quad (10)$$

where

$$\Delta T = T - T_{\text{predicted}},$$

T is the true temperature, and $n + 1$ the number of different wavelengths.

This equation states that the effects of measurement noise grow with the number of terms in the ratios, implying that two-color pyrometers are the most practical of the ratio pyrometers.

C. Reference temperature

In some systems of practical interest one may find a point in either time or space where the temperature is known, e.g., a fusion boundary. It would be useful to consider whether one may take advantage of this information to improve the accuracy of the temperature predictions.

The methodology here would be to calculate the emissivity ratio at the known temperature and then to use this ratio to calculate temperatures away from the reference point. Thus, for a two-color method to predict correct temperatures, the emissivity ratio away from the reference point must remain equal to the value calculated at the reference point.

To analyze this approach we need to be concerned with the temperature dependent behavior of emissivity at a constant wavelength, i.e., we need to examine functions of the sort

$$\epsilon_1 = f_{\lambda_1}(T), \quad \epsilon_2 = f_{\lambda_2}(T).$$

For many systems of interest the emissivity is a linear function of temperature so that we can say

$$\epsilon_1 = m_1 T + b_1, \quad \epsilon_2 = m_2 T + b_2.$$

For such a system we can show that

$$\Delta T \text{ monotonic function of } \Gamma = (m_1/m_2) - (b_1/b_2), \quad (11)$$

where ΔT is the difference between the predicted and the actual temperatures.

Similar relations can be derived for emissivities with higher-order temperature dependencies, but this shall suffice to illustrate our point here.

D. Computer simulation

To examine the effects of different emissivities and noise levels, etc., a set of computer simulations were performed. Input data for the simulations were generated by calculating theoretical (Planck) black body radiances and then multiplying these by typical emissivity values for various metals. These data were then multiplied by a pseudorandom number to simulate the effects of noisy measurements.

The emissivity data were extracted from the published literature⁷⁻¹⁵ and curve fit to various polynomials and exponential polynomials. Table I lists the coefficients of these polynomials, where

$$\text{Emissivity}(\lambda) = \sum_{i=0}^{m-1} \alpha_i \lambda^i$$

and

$$\text{Emissivity}(\lambda) = \exp \left(\sum_{i=0}^{m-1} \alpha_i \lambda^i \right).$$

Figure 1 shows the match between the fitted functions and then the actual data for some of these metals.

These generated data were then used with the equations of the previous section to predict temperatures. Emissivity values from the literature were also introduced directly (without prior fitting) but these did not give significantly different results.

TABLE I. Fitting parameters for emissivity data of several materials from the literature.

Emissivity code number	Material	Coefficients	
		Polynomial	Exponential
0	Black body	$a_0 = 1.000$	
1	Cadmium	$a_0 = 1.330$ $a_1 = -1.636$ $a_2 = 1.809$ $a_3 = -0.606$	
2	Chromium	$a_0 = 0.773$ $a_1 = -1.37$ $a_2 = 1.524$ $a_3 = -0.539$	
3	Iron 1	$a_0 = 0.755$ $a_1 = -0.971$ $a_2 = 0.9323$ $a_3 = -0.337$	$a_0 = -0.361$ $a_1 = -0.667$
4	Iron 2	$a_0 = 0.35$ $a_1 = 0.672$ $a_2 = -1.220$ $a_3 = 0.547$	
5	Nickel	$a_0 = 1.05$ $a_1 = -2.321$ $a_2 = 2.424$ $a_3 = -0.872$	
6	Platinum 1	$a_0 = 1.3485$ $a_1 = -3.1724$ $a_2 = 3.1142$ $a_3 = -1.0527$	$a_0 = -0.793$ $a_1 = -0.554$
7	Platinum 2	$a_0 = 0.8283$ $a_1 = -0.9073$ $a_2 = 0.3133$	
8	Molybdenum	$a_0 = 0.4950$ $a_1 = -0.0910$ $a_2 = -0.0033$ $a_3 = -0.1680$	$a_0 = 0.0892$ $a_1 = -1.0435$
9	Lead		$a_0 = -0.056$ $a_1 = -0.909$
10	Tantalum	$a_0 = 0.910$ $a_1 = -0.655$	$a_0 = -0.642$ $a_1 = -2.103$

E. Systems with a reference point

To simulate the occurrence of a reference point in the system under observation the following algorithm was devised:

1. Pick a temperature profile.
2. Pick two of the following emissivity-temperature dependencies: Linear (positive slope); Linear (negative slope) quadratic.
3. Generate radiance profile.
4. Add noise.
5. Calculate the emissivity ratio at the known temperature.
6. Use the emissivity ratio to calculate the temperature at other points.

It should be pointed out that this method will only yield an advantage if the system under observation is not a gray body at the reference temperature. There is evidence^{16,17} that at least some metals exhibit gray body behavior at their melting point.

F. Results and discussion

Figures 2 through 4 present the results of some of the simulations for two-, three-, and four-color ratio pyrometers for a target temperature of 1000 K. These results were generated with zero noise and using a wavelength separation of 12.5 nm. The similarity in the results of the different techniques shows that there is no advantage in using more than two colors for a ratio technique even in the absence of measurement noise.

There are two interesting aspects to these curves, namely the fact that none of the emissivities gives an error less than about 4%, and all of the predicted temperatures tend towards asymptotic behavior at some wavelength. Both of these facts are in complete agreement with the theory presented earlier. The minimum error behavior occurs because the constant emissivity assumption is never satisfied. The asymptotic behavior, on the other hand, can be explained by examining Eq. (9) in greater detail.

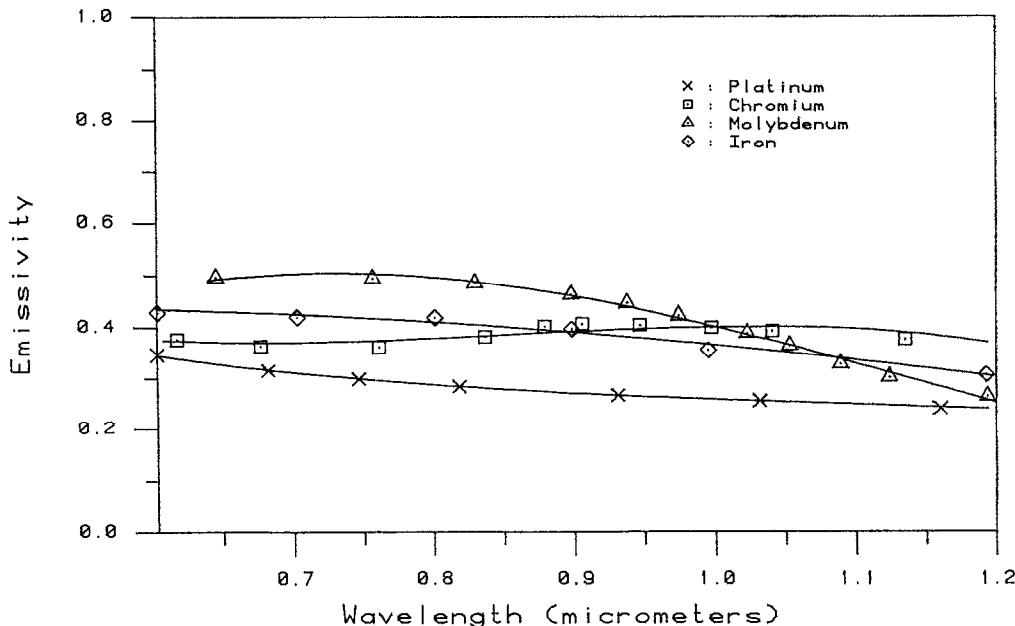


FIG. 1. Experimental emissivity data and the appropriate fitted curves.

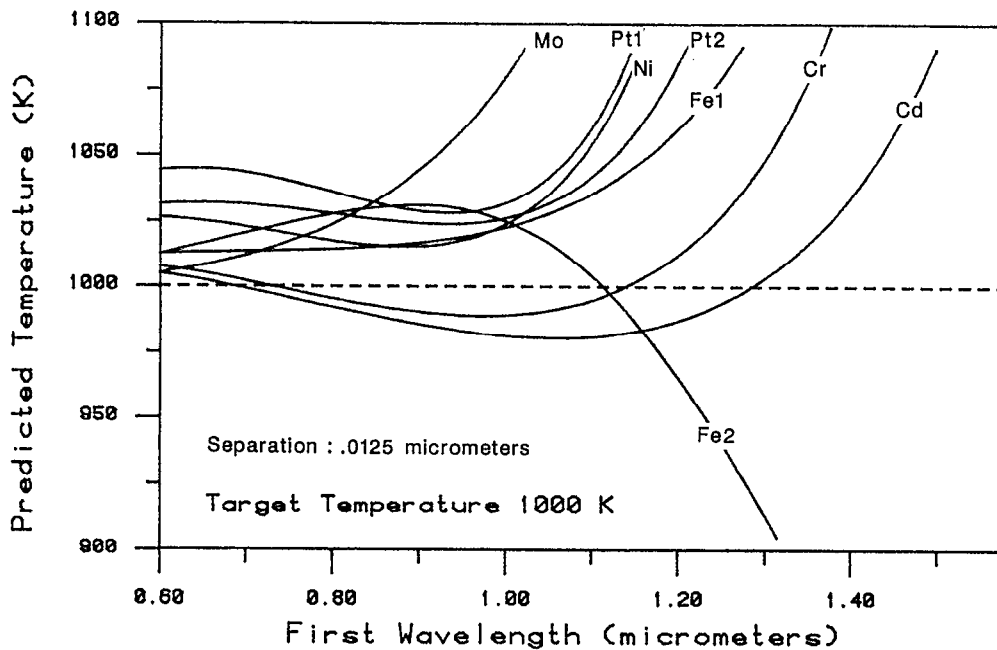


FIG. 2. Temperature predictions using a two-color method (zero noise).

In examining Eq. (9) we should recognize that emissivity and wavelength are not independent; in fact,

$$\epsilon = f(\lambda).$$

So for a specific material over a specific wavelength range we are not free to pick any values for K . Specifically for the materials considered here (Table I) we get the following ranges for K :

- Cr - $0.1 < K < +0.1$,
- Pt1 - $0.4 < K < -0.1$,
- Mo - $0.5 < K < -0.1$,
- Fe2 - $0.2 < K < 0.05$.

We now turn our attention to the partial derivatives of Eq. (9). Figure 5 is a plot of these quantities versus K . We can see that the $\Delta\epsilon$ and $\Delta\lambda$ derivatives can be the dominating terms in this equation depending upon the value of K . This implies that the critical factor in determining the behavior of T_a is K . This assertion is borne out by Fig. 6 which depicts the behavior of the predicted temperature (T_a) versus wavelength for various values of K . Of course this comes as no surprise if we keep in mind that in the limit as $\Delta\lambda \rightarrow 0$, K is just the slope of the emissivity with respect to λ .

If K is indeed the controlling influence on T_a , then the magnitude of the wavelength separation ($\Delta\lambda$) should have a minor effect on the accuracy of the temperature prediction.

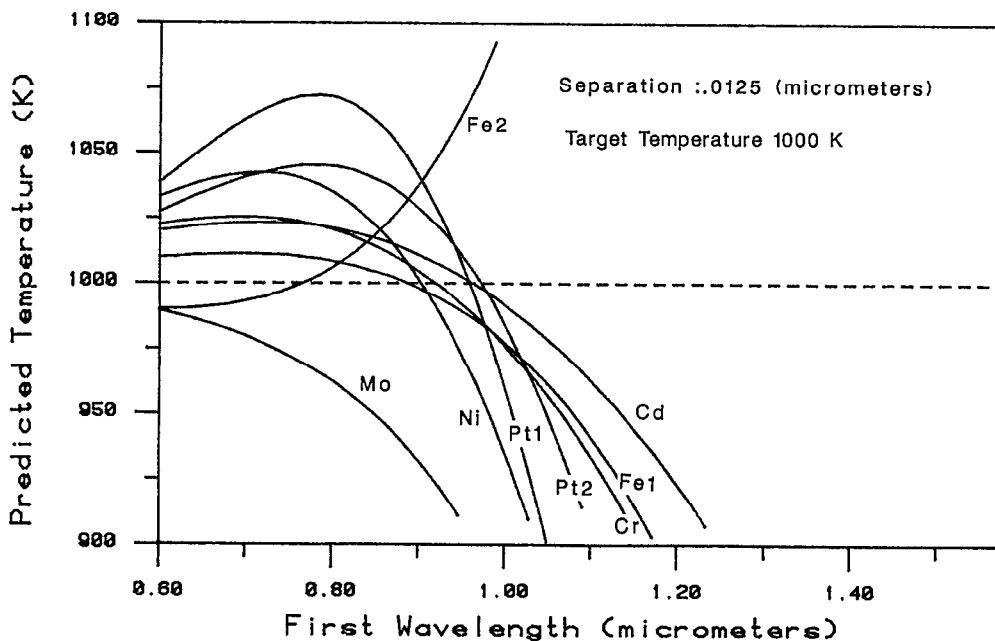


FIG. 3. Temperature predictions using a three-color method (zero noise).

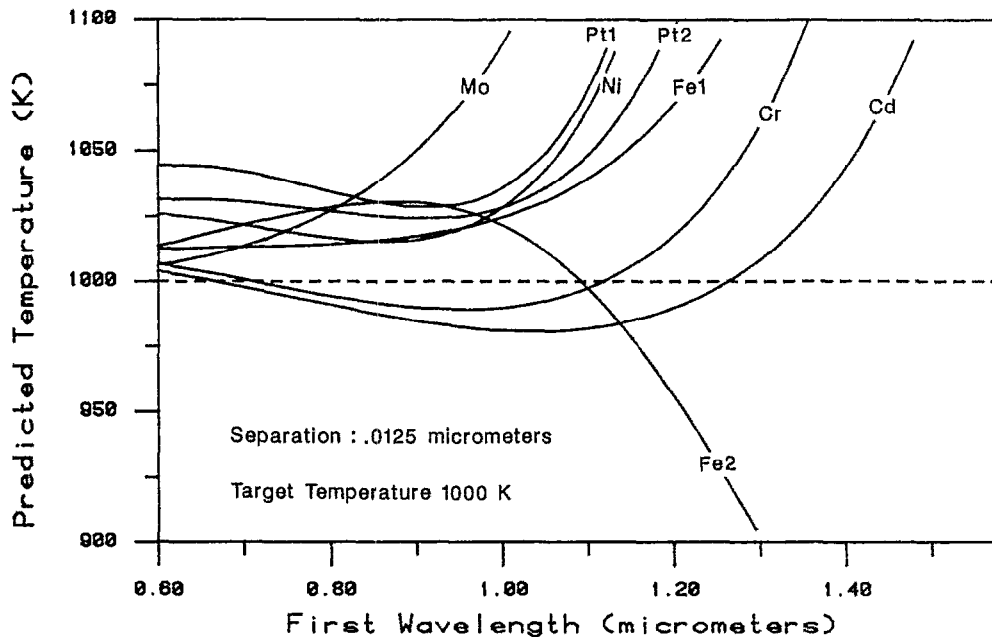


FIG. 4. Temperature predictions using a four-color method (zero noise).

The preceding statement assumes that changing $\Delta\lambda$ does not change K appreciably and that we are dealing with noiseless data. This is demonstrated by Figs. 7(a) and 7(b) which depicts the predicted temperature for Cr and Mo for various values of $\Delta\lambda$.

Similar results were obtained at a target temperature of 1800 K.

G. Effects of noise

The addition of noise to the input data makes the uncertainty of each temperature prediction considerably worse. As depicted in Fig. 8 even the addition of 0.2%-rms noise causes a significant increase in the uncertainty in the predict-

ed temperature. Additionally the three and four color ratio (not shown here) simulations predicted temperatures that respond in a progressively worse manner to the addition of noise.

H. Reference temperature

The reference temperature simulations were performed on a decreasing and an increasing temperature profile. As expected the error between the predicted and target temperatures is directly proportional to the quantity Γ (see Table II) described in the theory section.

The largest error above was caused by pairing a linear emissivity-temperature dependence with a quadratic depen-

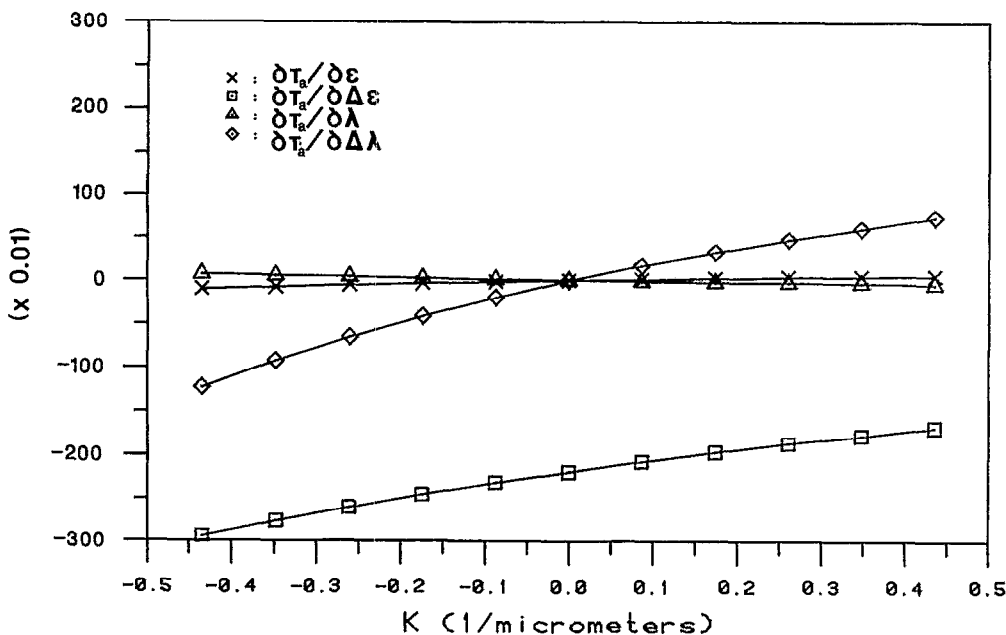


FIG. 5. The partial derivatives of T_e vs K .

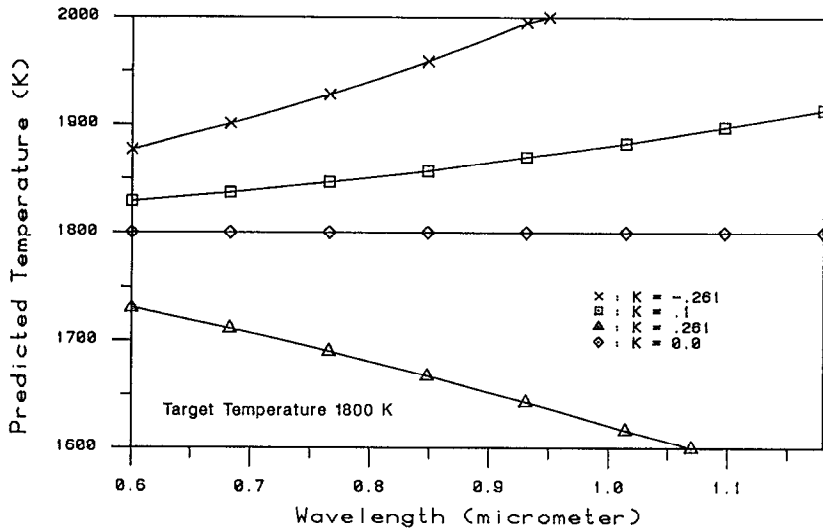


FIG. 6. Effect of K on the predicted temperature T_o (two color).

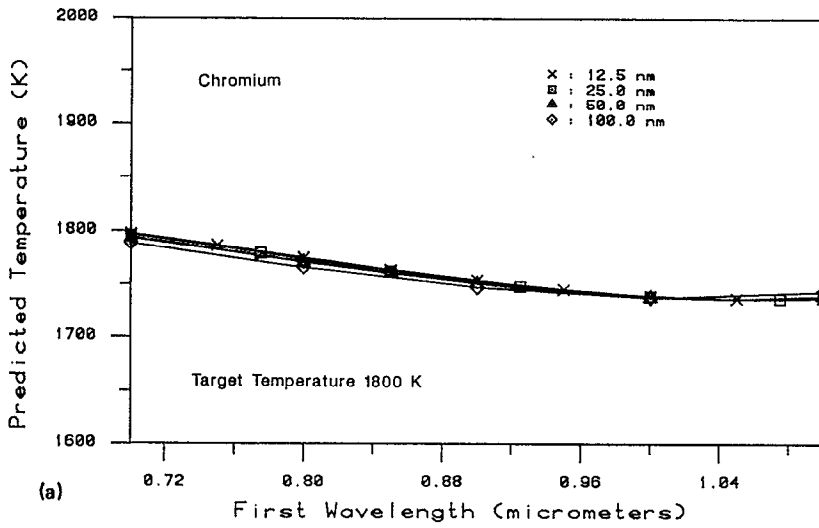
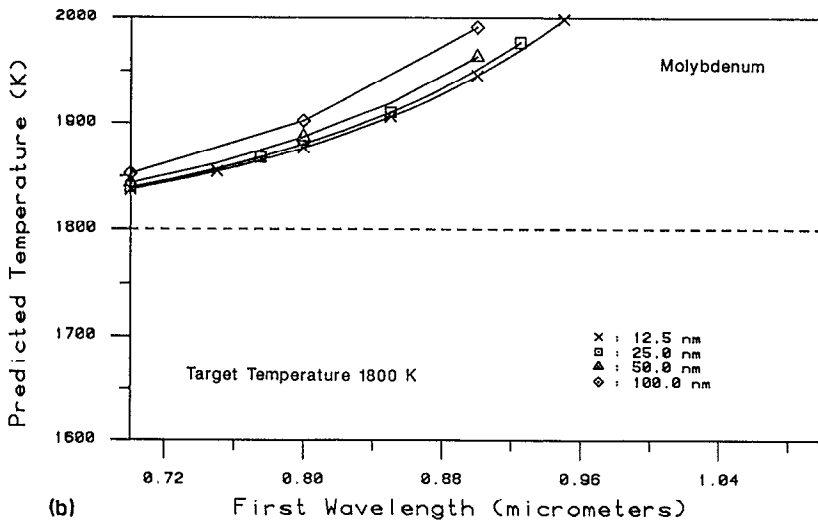


FIG. 7. Effect of changes in the wavelength separation on the two-color temperature prediction for (a) Cr, (b) Mo.



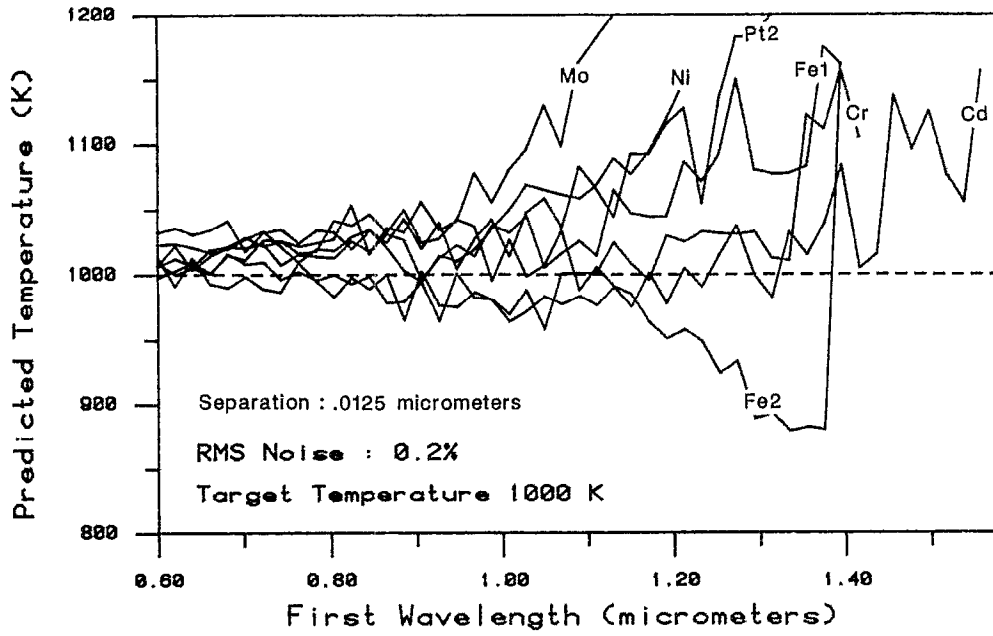


FIG. 8. Predicted temperature using a two color method on noisy (0.2%) data at 1000 K.

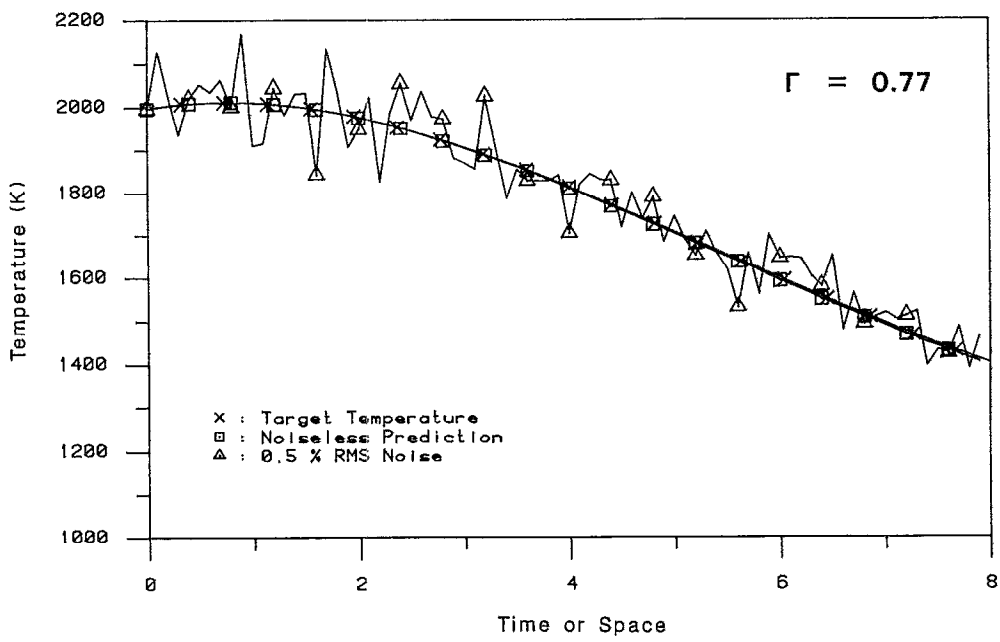


FIG. 9. Actual and predicted temperature profiles away (in time or space) from a reference point $\Gamma = 0.77$.

TABLE II. Temperature error as a function of emissivity slope mismatch.

Temperature error (K)	Γ
200	6.8
60	1.0
10	0.77

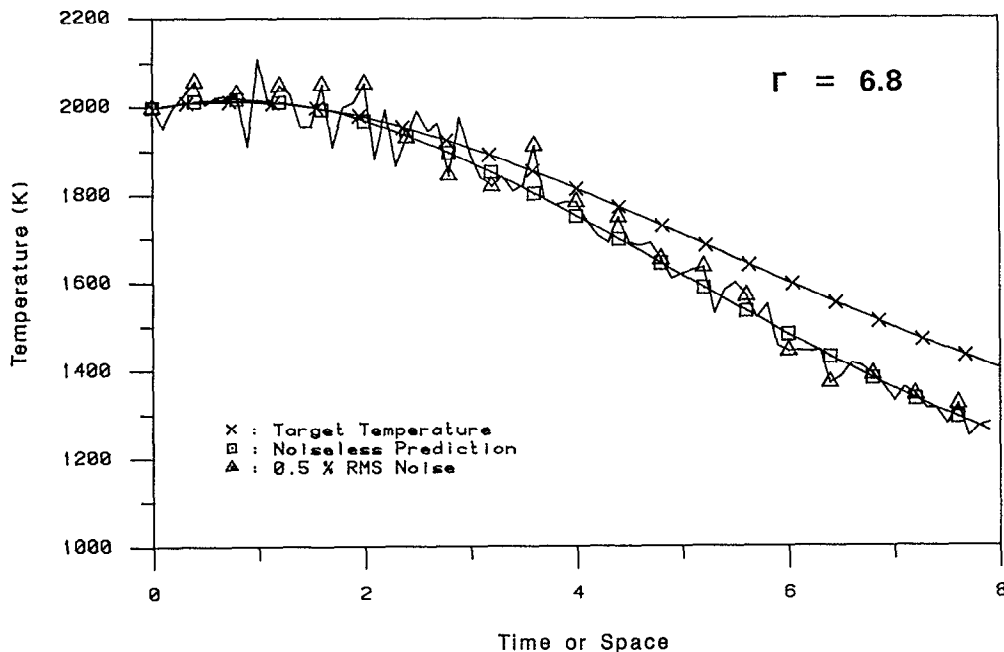


FIG. 10. Actual and predicted temperature profiles away (in time or space) from a reference point $\Gamma = 1.0$.

dence. Figures 9–11 depict the results of these simulations.

The addition of 0.5% rms random noise does not affect the results too badly. The over all uncertainty in the predictions does go up as a result of the noise, but the average value is not affected too much.

III. DISCUSSION

The method of ratio pyrometry has been shown to result in extremely large errors under certain conditions. These conditions can arise quite frequently as demonstrated by the simulations performed here. This method is better suited to the shorter wavelengths. The predicted temperature tends to

blow up (i.e., has an asymptote) for all the emissivity functions examined here.

Ratio pyrometry methods are also very sensitive to measurement noise. This sensitivity grows quickly with the number of terms in the ratio. Thus, it is recommended that if ratio pyrometry is to be used one should choose the two-color method over methods employing higher ratios.

If the emissivity of the object system meets certain constraints and the system has, in space or time, a point where the temperature is known, then the two-color method can be used to get very accurate temperature measurements away from this reference point. This technique can yield better

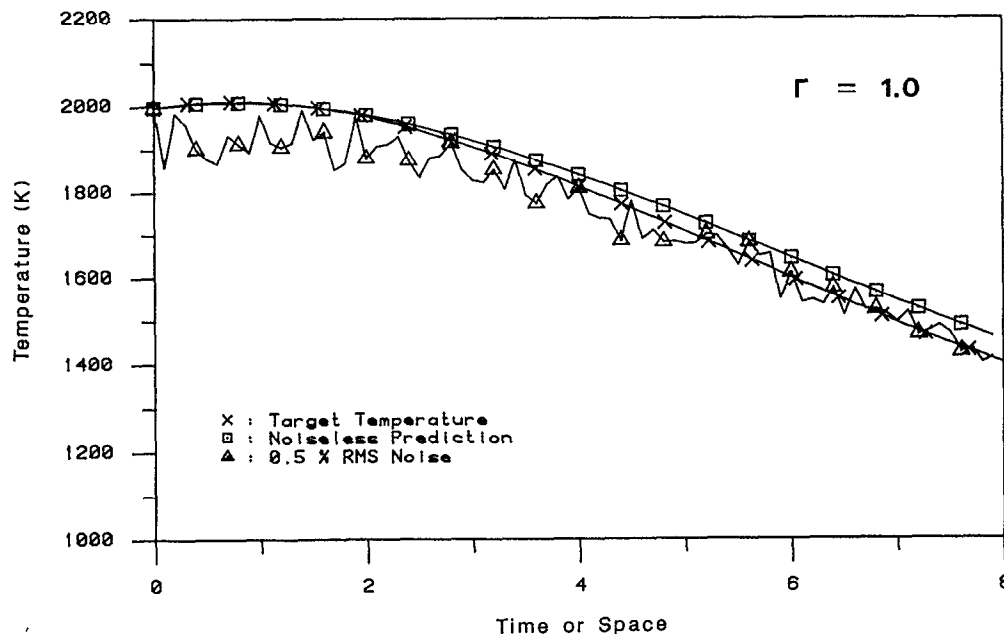


FIG. 11. Actual and predicted temperature profiles away (in time or space) from a reference point $\Gamma = 6.8$.

results (than a regular two-color method) if the emissivity of the system being observed is not wavelength independent at the known temperature.

ACKNOWLEDGMENT

The authors would like to acknowledge the Office of Naval Research for support of this work under Contract No. N00014-80-C-0384.

¹D. Ya. Svet, *High Temp.-High Press.* **4**, 715 (1972).

²D. Ya. Svet, *Sov. Phys. Dokl* **20**, 214 (1975).

³D. Ya. Svet, *Sov. Phys. Dokl* **21**, 162 (1976).

⁴P. B. Coates, *Metrologia* **17**, 103 (1981).

⁵P. M. Reynolds, *Br. J. Appl. Phys.* **15**, 579 (1964).

⁶G. B. Hunter, *Spectrometric Temperature Measurements of Thermal Radiators*, Ph.D. Thesis, MIT, Cambridge (1984).

⁷R. C. Weast and M. J. Astle, *Handbook of Chemistry and Physics* (CRC, Boca Raton, FL, 1979).

⁸S. Roberts, *Phys. Rev.* **114**, 104 (1959).

⁹T. Mori, K. Fujimura, T. Higashi, and H. Yoshimoto, *Iron and Steel* **57**, 1198 (1971).

¹⁰D. K. Edwards and N. B. de Volo (S. Gratch Co, ASME, New York, 1965).

¹¹W. E. Forsythe and E. Q. Adams, *JOSA* **35**, 108 (1945).

¹²S. R. Siegel, J. R. Howell, *Thermal Radiation Heat Transfer* (McGraw Hill, 1981).

¹³G. A. W. Rutgers, *Handbuch der Physik* **26**, 143 (1958).

¹⁴R. D. Larrabee, *JOSA* **49**, 619 (1959).

¹⁵G. G. Gubareff, J. E. Janssen, and R. H. Torborg, *Thermal Radiation Properties Survey*, Honeywell Research Center, Minneapolis, MI, 1960.

¹⁶J. P. Hiernaut, R. Beukers, W. Heinz, R. Selfslag, M. Hoch, and R. W. Ohse, *High Temp.-High Press.* **18**, 617 (1986).

¹⁷J. P. Hiernaut, R. Beukers, M. Hoch, T. Matsui, and R. W. Ohse, *High Temp. High Press.* **18**, 627 (1986).